

How to detect gap nodes of a superconductor by angle-resolved specific heat experiment?

P. Miranović

Department of Physics, University of Montenegro, 81000 Podgorica, Serbia and Montenegro

M. Ichioka and K. Machida

Department of Physics, Okayama University, Okayama 700-8530, Japan

N. Nakai

Yukawa Institute for Theoretical Physics, Kyoto University, Kyoto 606-8502, Japan

(Dated: February 2, 2008)

The specific heat oscillation in the mixed state of type II superconductors is studied theoretically when rotating field within a plane containing gap minimum and maximum. The calculations are performed microscopically by solving quasi-classical Eilenberger equation for vortex lattices. The field dependence of the oscillation amplitude can discriminate between the nodal and anisotropic gap with a finite minimum and the oscillation phase gives the gap minimum position on the Fermi surface. These also provide a way to separate out the anisotropic behavior due to the Fermi velocity.

PACS numbers: 74.25Bt, 74.25Op, 74.20Rp

I. INTRODUCTION

There has been much attention focused on exotic superconductors, including high T_c cuprates and heavy Fermion materials in recent years. In addition to the spin structure or parity of the Cooper pair, the orbital function or the gap structure on the Fermi surface is decisive to characterize its superconductivity. These studies are expected to lead to a new pairing mechanism. Even in conventional superconductors the energy gap can vary, depending on the position on the Fermi surface. The degree of the anisotropy in the gap function is an important factor in understanding a superconductor in question. To distinguish a nodal superconductor from an anisotropic one with a finite minimum gap is of particular importance because the gap function can not change its sign in the latter while it can in the former. Also it is crucial to determine the maximum and minimum gap positions on the Fermi surface.

It is now widely recognized that the zero-energy density of states (ZEDOS) sensitively reflects the gap structure, which is probed by a variety of experimental methods such as specific heat, thermal conductivity or scanning tunneling spectroscopy. This is particularly true for physical quantities in the mixed state of type II superconductors. Induced vortices under an applied field carry a certain amount of ZEDOS around each vortex core which depends on the gap structure^{1,2,3}. The Sommerfeld coefficient $\gamma(B)$ as a function of magnetic induction B , which is nothing but ZEDOS induced by vortices, is found to be one of physical quantities to reveal the gap topology. In fact, there have been several $\gamma(B)$ experiments^{4,5,6,7,8,9} on such as 2H-NbSe₂, V₃Si, Nb₃Sn or CeRu₂. We recently demonstrate that precise measurement $\gamma(B)$ at low field gives rise to indispensable information on the gap anisotropy¹⁰. In order to better characterize the gap

structure it is urgent to provide further ways to analyze experimental data. For example, anisotropic behaviors in a superconductor could come from the two main sources. One is the gap structure itself and the other is the Fermi velocity anisotropy due to band structure. It is often the case that these two kinds of anisotropy are mixed up and difficult to separate out individually, leading to an ambiguous conclusion as for the gap structure. Thus we are required to devise some method to disentangle these two anisotropy effects.

Recently the angle-dependent specific heat experiments for the mixed state in several superconductors LuNi₂B₂C 11, CeCoIn₅ 12 and Sr₂RuO₄ 13 have been performed to yield characteristic oscillation pattern in $\gamma(B)$. A few percent oscillation amplitude relative to the total in these experiments is generally consistent with the theoretical estimate³ for nodal superconductors or strongly anisotropic gap superconductors. However, it remains open to distinguish between them. Specifically, it is reported that the oscillation amplitude becomes vanishing toward $B \rightarrow 0$ in Sr₂RuO₄ 13 while it remains a finite value in LuNi₂B₂C 11 and CeCoIn₅ 12. It was speculated that in the former either the gap structure has a finite minimum gap or the gap in the minor band may mask the oscillation in lower fields. Thus we need to know precise behavior of the field-dependence of the oscillation amplitude for the two cases.

The purpose of the present paper is to examine the oscillation amplitude of the angle-dependent Sommerfeld coefficient $\gamma(B)$ when B rotates within a plane containing the gap minimum and maximum for several typical gap topologies, including line and point node superconductors and a superconductor with a finite minimum gap. We also study the oscillation behavior of $\gamma(B)$ for isotropic gap case with the anisotropic Fermi velocity. It turns out that this anisotropy also yields a substantial specific heat oscillation under field rotation, but we will

provide information on how to distinguish it from the gap anisotropy case. The existing data of the $\gamma(B)$ oscillation experiments on $\text{LuNi}_2\text{B}_2\text{C}$, CeCoIn_5 and Sr_2RuO_4 are analyzed in this regard. After a brief introduction to quasi-classical framework to show how to calculate the ZEDOS for various situations, we describe the results of the ZEDOS oscillations to examine the differences between node versus nodeless gap cases in Section 3 and also show the results for anisotropic Fermi velocity in Section 4. The Section 5 is devoted to the point node case in comparison with the line node case to supplement the above analysis. In the Section 6 we give a summary and discussions on the existing data. All computations are done assuming a Fermi sphere.

II. QUASI-CLASSICAL THEORY AND ZEDOS

The amplitude of the specific heat oscillations appears to be very small, just few percents^{11,12,13} as mentioned before. The smallness of the effect necessitates the use of numerical solutions of Gorkov's microscopic equations of superconductivity to accurately estimate the specific heat amplitude. Quasi-classical approximation of Gorkov's equations, that we solve numerically here, is good as long as condition $k_F\xi \gg 1$ is met. Here, k_F^{-1} is in the order of atomic length, and ξ is coherence length. Pairing interaction between electrons is modeled as $V(\mathbf{v}, \mathbf{v}') = V_0\Omega(\mathbf{v})\Omega(\mathbf{v}')$. This greatly simplifies the analysis, since pairing potential in this model can be written as $\Delta(\mathbf{r}, \mathbf{v}) = \Omega(\mathbf{v})\Psi(\mathbf{r})$. The orbital part of the pairing potential, $\Omega(\mathbf{v})$, we simply call: the gap function. Eilenberger equations then read as ($\hbar = 1$)

$$[2\omega + \mathbf{v}\Pi] f(\omega, \mathbf{r}, \mathbf{v}) = 2\Delta(\mathbf{r}, \mathbf{v})g(\omega, \mathbf{r}, \mathbf{v}), \quad (1)$$

$$[2\omega - \mathbf{v}\Pi^*] f^\dagger(\omega, \mathbf{r}, \mathbf{v}) = 2\Delta^*(\mathbf{r}, \mathbf{v})g(\omega, \mathbf{r}, \mathbf{v}). \quad (2)$$

Here $\Pi = \nabla + (2\pi i/\Phi_0)\mathbf{A}$ is gauge invariant gradient, \mathbf{A} is vector potential, Φ_0 is flux quantum, $\mathbf{v} = \mathbf{v}(\mathbf{k}_F)$ is Fermi velocity defined as $\mathbf{v}(\mathbf{k}) = \nabla_{\mathbf{k}}E(\mathbf{k})$, with $E(\mathbf{k})$ being energy function of electrons in band; Fermi wave vector \mathbf{k}_F can be found from the equation $E(\mathbf{k}) = E_F$; $\omega = \pi T(2n+1)$ with integer n is Matsubara frequency, g and f are normal and anomalous Green's function and $f^\dagger(\omega, \mathbf{r}, \mathbf{v}) = f^*(\omega, \mathbf{r}, -\mathbf{v})$. Normalization condition for the Green's functions is $g^2 + f f^\dagger = 1$.

The selfconsistency equations for the gap function and current density are:

$$\Delta(\mathbf{r}, \mathbf{v}) = 2\pi N_0 T \sum_{\omega>0} \int_{FS}^{\omega_D} d^2k'_F V(\mathbf{v}, \mathbf{v}') \rho(\mathbf{k}'_F) f, \quad (3)$$

$$\mathbf{j} = 4\pi i |e| N_0 T \sum_{\omega>0} \int_{FS} d^2k_F \rho(\mathbf{k}_F) \mathbf{v} g. \quad (4)$$

Here, \int_{FS} is integral over the Fermi surface, ω_D is cut off frequency, N_0 is the total density of states for one spin at the Fermi surface in the normal state

$$N_0 = \int_{FS} \frac{d^2k_F}{(2\pi)^3} \frac{1}{|\mathbf{v}|}, \quad (5)$$

and $\rho(\mathbf{k}_F)$ is the angle resolved density of states at the Fermi surface:

$$\rho(\mathbf{k}_F) = \frac{1}{(2\pi)^3 N_0} \frac{1}{|\mathbf{v}|}, \quad (6)$$

normalized so that:

$$\int_{FS} d^2k_F \rho(\mathbf{k}_F) = 1. \quad (7)$$

Density of states $N(\mathbf{r}, E)$ is defined as

$$N(\mathbf{r}, E) = N_0 \int_{FS} d^2k_F \text{Re } g(i\omega = E + i\delta, \mathbf{r}, \mathbf{v}) \rho(\mathbf{k}_F) \quad (8)$$

We are interested in low temperature zero-energy density of states (ZEDOS) $N(\mathbf{r}, E = 0)$. This is because in the limit of small temperatures, $T \rightarrow 0$, ratio of specific heat in superconducting state C_s and normal state C_n is given by

$$\lim_{T \rightarrow 0} \frac{C_s}{C_n} = \frac{\overline{N(\mathbf{r}, E = 0)}}{N_0}. \quad (9)$$

Here $\overline{N(\mathbf{r}, E = 0)}$ is spatially averaged ZEDOS in superconducting state. In our calculation we set $T = T_c/10$. Since ZEDOS and specific heat are proportional at low temperatures we use these two terms concurrently throughout the text. Numerical procedure for solving quasi-classical equations of superconductivity is described in Ref. 19. Magnetic field is measured in units $\Phi_0/(2\pi R_0^2)$, where Φ_0 is flux quantum, and $R_0 = 0.882 \xi_0$ (ξ_0 is BCS coherence length).

Angular dependence of ZEDOS is already studied numerically for some typical cases of nodal gap function: 3D d-wave, polar state, and axial state³. Also, ZEDOS is studied by using the high field approximate solution of Eilenberger equations^{14,15,16,17,18}. The focus in that study was on field dependence of ZEDOS for characteristic magnetic field directions. Just to recall, as one rotates magnetic field from the gap node direction toward gap maximum direction, ZEDOS increases in low field, while it decreases in fields near H_{c2} . In other words, specific heat oscillation amplitude changes sign with increasing field. In this paper we compare ZEDOS oscillation amplitude for nodal and nodeless superconductors in the limit of low fields. Along with the nodal gap structures already studied in Ref. 3, we present also results for some other typical cases known in the literature.

III. NODAL GAP VS NODELESS GAP

In order to distinguish the nodal gap superconductor from the nodeless superconductor with a finite minimum gap, we examine the following model for the gap structure

$$\Omega(\varphi, \theta) = \Omega_0(a) \sqrt{1 + a \cos 4\varphi} \quad (10)$$

with φ polar angle and θ azimuthal angle in polar coordinates. The parameter a measures the degree of anisotropy. For $a = 0$ the gap function is isotropic, while for $a = 1$ the gap function reduces to two-dimensional (2D) version of $d_{x^2-y^2}$ -wave superconductivity. We choose the prefactor $\Omega_0(a)$ so that the average of Ω^2 over the Fermi surface is unity, independent of a . ZEDOS is calculated for fields rotating in the basal plane with $\theta = \pi/2$. Only two field directions are of our interest, B along the gap minimum ($\varphi = (2k+1)\pi/4$), and B along the gap maximum ($\varphi = k\pi/2$). Here, k is integer. We performed the calculation for two anisotropy parameters: $a = 0.5$ and $a = 1$. In both cases, low field ZEDOS is always minimum when the magnetic field is oriented along the gap minimum (node) and vice versa.

In Fig. 1 the ratio $R = N(E = 0, \varphi = 0)/N(E = 0, \varphi = \pi/4)$ of maximum and minimum ZEDOS, for field rotating in the basal plane, is plotted for both anisotropy parameters. As is clear from Fig. 1, there is a striking difference in low field dependence of ratio R for nodal $a = 1$ and nodeless $a = 0.5$ superconducting gap. Namely, for the nodal gap case ($a = 1$) there is a finite amplitude ZEDOS oscillation ($R \neq 1$) towards $B \rightarrow 0$. This is contrasted with the nodeless gap case ($a = 0.5$) where R becomes unity at lower fields, showing a maximum at the intermediate field region B_{max} . This means that the specific heat oscillation diminishes there. The field

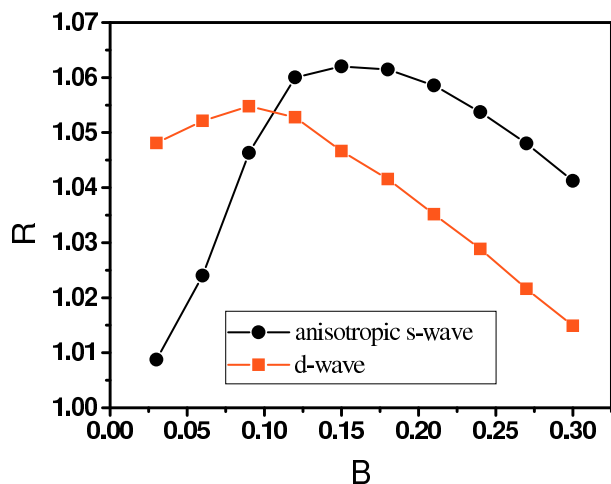


FIG. 1: Ratio $R = N(E = 0, \varphi = 0)/N(E = 0, \varphi = \pi/4)$ of minimum and maximum ZEDOS for fields rotating in the basal plane of the crystal. Full circles are for anisotropy parameter $a = 0.5$, while full squares are for 2D d -wave superconductor ($a = 1$).

B_{max} comes from the physical reason that at $B < B_{max}$ the spatial extension of the ZEDOS is confined to each vortex core region, yielding more or less isotropic ZEDOS landscape. This ZEDOS feature does not cause the specific heat oscillation in this lower field. The spatial extension of the ZEDOS landscape depends on the size of the minimum gap because the gap acts as a potential for quasi-particles, that is, the zero-energy quasi-particles are strongly confined and localized near each core. Thus B_{max} signals the characteristic field where the localized zero-energy quasi-particles begin overlapping and tends to become smaller as the minimum gap decreases. Since in the nodal gap case the spatial extension of the ZEDOS is extended to infinity, B_{max} approaches zero, indicating that R stays a constant towards smaller fields.

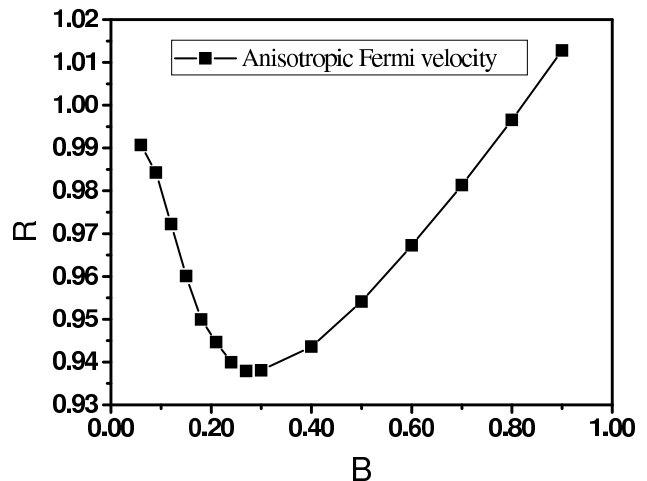


FIG. 2: Ratio $R = N(E = 0, \varphi = 0)/N(E = 0, \varphi = \pi/4)$ of minimum and maximum ZEDOS in case of anisotropic Fermi velocity modeled by Eq. (11).

IV. ANISOTROPIC FERMİ VELOCITY

We analyze the other type of anisotropy. The superconducting gap is assumed to be isotropic, or to have the same value all over the Fermi surface, but the Fermi velocity itself is anisotropic. The amplitude of the Fermi velocity on the Fermi sphere is modeled as:

$$v(\varphi, \theta) = v_0(b)(1 + b \cos 4\varphi). \quad (11)$$

The parameter b measures the degree of anisotropy. For convenience the prefactor $v_0(b)$ is chosen so that density of states in normal state is independent of b . Four-fold variation of the Fermi velocity in the basal plane is a quite simple model but will suffice for our purpose. Even in this hypothetical case with the isotropic gap and the anisotropic Fermi velocity, ZEDOS, and thus specific heat, depend on magnetic field direction. In Fig. 2, we plot the ratio R of minimum and maximum ZEDOS as a function of magnetic field. The anisotropy parameter

$b = 0.5$ is used in the calculation. The ratio R between maximum and minimum ZEDOS is of the order of a few percent. This is the same order of magnitude as in the above gap anisotropy cases. This is also the same order of magnitude observed¹¹ in $\text{LuNi}_2\text{B}_2\text{C}$. This warns us that the effect of the Fermi surface structure on the specific heat oscillation cannot be neglected in intermediate fields. However, it is seen from Fig. 2 that extrapolation of maximum/minimum ratio R to $B = 0$ gives $R = 1$, i.e. disappearance of specific heat oscillation. This is qualitatively the same behavior as seen in the anisotropic gap case with a finite minimum gap, shown in Fig. 1. Physically this is due to the spatial extension of the zero-energy quasi-particle state: In the Fermi velocity anisotropy case ZEDOS is confined to each core in a rather isotropic gap manner. Thus to induce the oscillation finite field is needed, above which because of the overlapping of the zero-energy quasi-particles, ZEDOS begins to exhibit an oscillation.

It is also noticed that in the above $b > 0$ case $R < 1$, meaning that the four-fold oscillation pattern is maximally phase-shifted by $\pi/4$ from the gap anisotropy cases with $R > 1$ in Fig. 1. Needless to say, the sign b is arbitrary for a given material, but it is physically plausible case $b > 0$ when $a > 0$ because in the angle-resolved DOS $N(\varphi) \propto 1/v(\varphi)$ the larger energy gap ($\varphi = 0$) coincides with the larger angle-resolved DOS. This is indeed the case in boro-carbides. Therefore, we can clearly distinguish the two anisotropy effects by measuring the angle-dependent specific heat to monitor both the oscillation amplitude and its phase.

V. POINT NODE GAP

In this section we consider the point node gap structure. Among several possible point node topologies we take up typical examples, the so-called axial state and “s+g” model. The former is known to be realized in superfluid ^3He A phase and the latter is an candidate for boro-carbides²⁰. We also consider the polar state with a line node for comparison.

A. Axial and polar gap function

The polar gap function has a horizontal line node in the crystal basal plane, while the axial gap function is characterized by two point-like nodes at the poles of the Fermi sphere. In polar coordinates with φ and θ denote polar and azimuthal angle, then the polar gap function is presented with

$$\Omega(\varphi, \theta) = \sqrt{3} \cos \theta, \quad (12)$$

and the axial gap function is presented with

$$\Omega(\varphi, \theta) = \sqrt{3/2} \sin \theta. \quad (13)$$

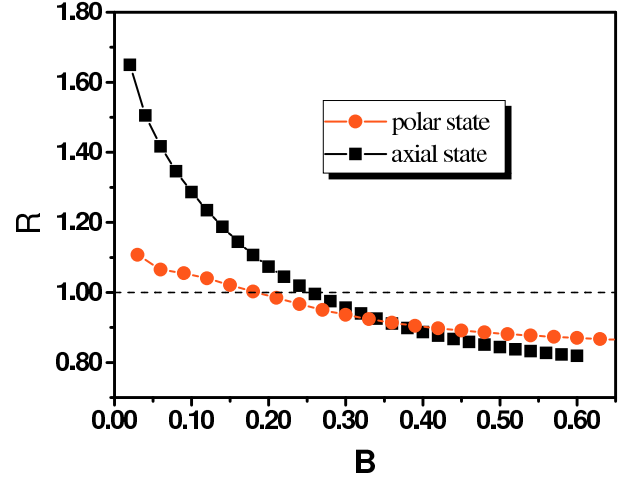


FIG. 3: Ratio $R = N(E = 0, \text{antinodal})/N(E = 0, \text{nodal})$ as a function magnetic induction for polar and axial gap function.

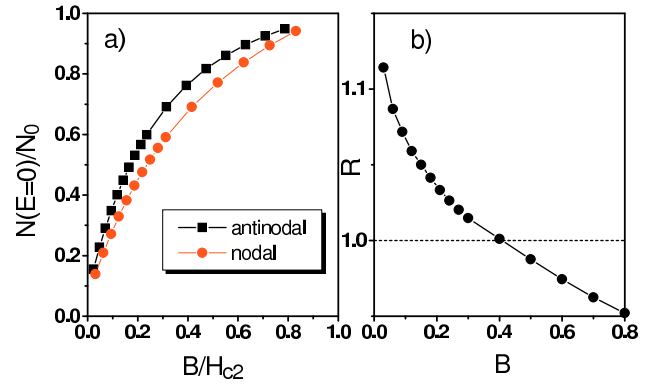


FIG. 4: a) Field dependence of ZEDOS for two field directions: nodal and antinodal when fields are rotated in the basal plane. b) Ratio $R = N(E = 0, \text{antinodal})/N(E = 0, \text{nodal})$ as a function magnetic induction.

The low temperature ZEDOS for these two gap functions is studied in detail in Ref. 3. By rotating magnetic field in a plane that contains c -axis, ZEDOS periodically changes. The ZEDOS maximum appears for the field oriented along the gap node, and the ZEDOS minimum appears when magnetic field is directed along the gap maximum. Although field dependence of ZEDOS is already presented in Ref. 3, for the purpose of this paper we present those data in a slightly different form. Namely, we are interested in the amplitude of ZEDOS oscillation as a function of B . Therefore, in Fig. 3 the field dependence of ratio $R = N(E = 0, \text{antinodal})/N(E = 0, \text{nodal})$ is shown. The low field ratio differs significantly for the axial and polar gap functions. The important point to notice is that in both cases ratio R , in the limit of low fields, differs from 1. This means that there is a finite amplitude of ZEDOS oscillation as $H \rightarrow 0$. This is in accord with the conclusion in the previous sections.

B. "s+g" model

It has been argued that the gap function in borocarbides is a mixture of s -wave and g -wave superconductivity with aptly chosen weighting factors so that the pairing potential $\Omega(\varphi, \theta)$ does not change sign on the Fermi surface but has point-like zeros:

$$\Omega(\varphi, \theta) = \sqrt{\frac{315}{379}} (1 - \sin^4 \theta \cos 4\varphi). \quad (14)$$

Like in previous examples of anisotropic pairing functions, we choose the Fermi surface as a sphere to see the effect of the gap structure on low temperature thermodynamics. As we have already shown, even the anisotropy of Fermi surface alone can account for direction dependent specific heat. The effect of Fermi surface disappears only in the limit of low fields. Having in mind that band structure in borocarbides is far from being isotropic, this simple "s+g" gap function on Fermi sphere, may not be an appropriate model which can accurately estimate the amplitude of specific heat oscillation in borocarbides, but we can gain qualitative tendency in this case. In Fig. 4a) the field dependence of low temperature zero-energy DOS is shown for nodal and antinodal field directions. We define the antinodal direction as a direction in the basal plane with maximum value of superconducting gap. Magnetic induction B is scaled with $H_{c2}(\text{antinodal})$ and $H_{c2}(\text{nodal})$ respectively. Note that $H_{c2}(\text{antinodal}) > H_{c2}(\text{nodal})$. As one may already anticipate, difference between the maximum ZEDOS (field along antinodal direction) and the minimum ZEDOS (field along nodal direction) remains finite in low fields. Thus their ratio $N(E = 0, \text{antinodal})/N(E = 0, \text{nodal}) \neq 1$. This is shown in Fig 4b). Noteworthy is comparison with gap structure of the axial state $\Omega(\varphi, \theta) = \sqrt{3/2} \sin \theta$. Both, the axial state and "s+g" model, have point like nodes, while their field dependence of ZEDOS is different. The $\gamma(B)$ behavior as a function of B is not governed only by the gap node topology, point-like or line-like nodes. It is not unique for all types of gap structures with point-like (or line-like) nodes. It rather reflects the gap value on average, and it is rather sensitive to the functional form of the gap function in the vicinity of node.

VI. DISCUSSIONS ON THE SPECIFIC HEAT EXPERIMENTS

In this section we discuss the angle dependent specific heat experiments on three materials, $\text{LuNi}_2\text{B}_2\text{C}$, CeCoIn_5 and Sr_2RuO_4 in the light of the present calculations.

A. Boro-carbides

Park *et al* measure the angle-dependent $\gamma(B)$ for $\text{LuNi}_2\text{B}_2\text{C}$ and detect the four-fold oscillations in var-

ious fields, identifying the gap minimum is located in [100] direction of tetragonal crystal because the oscillation maximum is in [110] direction. This identification is supported by our present result. The oscillation amplitude becomes smaller as B decreases. However, it is rather difficult to judge whether the gap has a node or a finite minimum gap from their experiment where the detailed low field data are lacking. In connection with other experiments which suggest strong anisotropic gap²¹ or point node gap²² in this system, it is interesting to extend their measurement to lower field to determine the precise gap structure.

Izawa *et al*²² show in their angle-dependent thermal conductivity measurement: (1) In the similar oscillation pattern the maximum appears in [110], coinciding with that in Park *et al*. (2) The oscillation amplitude diminishes when field rotates conically out of the basal plane. For the polar angle $\theta > \pi/4$ it almost vanishes. They conclude a point node gap located along [100] direction. This assertion is based on a theoretical calculation²⁰ of angle dependence of thermal conductivity. It may be informative in this connection to show our result: We have also performed the calculation²³ when field rotates conically to check how the oscillation amplitude varies as a function of the polar angle θ . It is found that it decreases quickly as θ increases from zero for both vertical line node and the "s+g" point node cases, being unable to distinguish these two cases by conical field rotation of specific heat experiment.

B. CeCoIn₅

Aoki *et al*¹² perform the angle dependent specific heat experiment in this system, observing a substantial oscillation amplitude when rotating field within the basal plane of tetragonal symmetry crystal. In the oscillation pattern the maximum occurs for [110] direction. This suggests the d_{xy} gap function because the oscillation amplitude stays constant towards lowest fields. This conclusion appears to be inconsistent with the angle-dependent thermal conductivity experiment by Izawa *et al*²⁴, who conclude the $d_{x^2-y^2}$ gap function. Note, however, that their data themselves exhibit the oscillation maximum for [110] direction, consistent with Aoki *et al*¹².

C. Sr₂RuO₄

According to Deguchi *et al*¹³, who measure the angle-dependent specific heat on this system by rotating field within the basal plane of tetragonal crystal, the four-fold oscillation amplitude decreases below a threshold field $\sim 0.3T$ and changes its sign near $B_{c2} \sim 1.5T$. The existence of the threshold field is in accord with our calculation where the gap structure has a finite minimum gap, definitely excluding the vertical line node in the so-called main γ band. (We can not say anything about

the possible horizontal line node²⁵.) An interesting point in this system is the fact that we know accurately the Fermi velocity anisotropy in the γ band, where the larger Fermi velocity is directed to [110]. Since the observed oscillation maximum occurs along [110], the experiment unambiguously excludes the oscillation due to the Fermi velocity anisotropy. Combining these two facts we conclude that there exists the anisotropic gap structure with a finite minimum in the basal plane of the main γ band in Sr_2RuO_4 . We can not commit ourselves on further conclusion concerning the minor α and β bands or the horizontal line node based on the existing data by Deguchi *et al*¹³.

VII. SUMMARY AND CONCLUSION

In this paper, we have calculated the zero-energy density of states in the mixed state at low temperature by employing quasi-classical Eilenberger formalism, which is valid for a wide variety of superconductors. We have focused on the angle dependence of the zero-energy density of states, which is directly measured through specific heat experiment as the Sommerfeld coefficient, for superconductors with both nodal or nodeless gap structures.

We have demonstrated that the specific heat angular dependence provides useful information concerning the gap structure, namely, the position of the node or the

gap minimum on the Fermi surface and also the existence or non-existence of the gap node. Furthermore, we give information to distinguish two sources of the anisotropy, either due to the gap itself or due to the Fermi velocity of band structure. These proposed methods, we believe, add yet another dimension to firmly establish the gap structure.

A few examples studied here does not exhaust all possibilities for superconducting gap function. Neither all kind of different Fermi surface structures can be covered. Nevertheless, from the comparison of field dependence of ZEDOS in: a) nodal, and b) fully gaped anisotropic superconductors, one can conjecture a behavior that is common for each group of superconductors. In nodal superconductors the specific heat oscillation amplitude persists down to very low fields. In contrast to this behavior, fully gapped superconductors, as one decreases magnetic field the oscillation amplitude gradually diminishes. To remind the reader again, only low temperature specific heat is discussed here.

VIII. ACKNOWLEDGMENTS

We are grateful for useful discussions and communication with Y. Matsuda, T. Sakakibara, K. Izawa, J. Sonier, K. Deguchi, Y. Maeno, A. Junod, and M. Salamon.

-
- ¹ G. E. Volovik, JETP Lett. **58**, 469 (1993).
 - ² M. Ichioka, A. Hasegawa, and K. Machida, Phys. Rev. B **59**, 8902 (1999). M. Ichioka, A. Hasegawa, and K. Machida, Phys. Rev. B **59**, 184 (1999).
 - ³ P. Miranović, N. Nakai, M. Ichioka, and K. Machida, Phys. Rev. B **68**, 052501 (2003).
 - ⁴ J. E. Sonier, M. F. Hundley, J. D. Thompson, and J. W. Brill, Phys. Rev. Lett. **82**, 4914 (1999).
 - ⁵ A. P. Ramirez, Phys. Lett. A **211**, 59 (1996).
 - ⁶ V. Guritanu, W. Goldacker, F. Bouquet, Y. Wang, R. Lortz, G. Goll, and A. Junod, cond-mat/0403590.
 - ⁷ M. Hedo, Y. Inada, E. Yamamoto, Y. Haga, Y. Onuki, Y. Aoki, T. D. Matsuda, H. Sato, and S. Takahashi, J. Phys. Soc. Jpn. **67**, 272 (1998).
 - ⁸ M. Nohara, M. Isshiki, F. Sakai, and H. Takagi, J. Phys. Soc. Jpn. **68**, 1078 (1999).
 - ⁹ A. Mirmelstein, A. Junod, E. Walker, B. Revaz, J. Y. Genoud, and G. Triscon, J. Supercond. **10**, 527 (1997).
 - ¹⁰ N. Nakai, P. Miranović, M. Ichioka, and K. Machida, cond-mat/0403589.
 - ¹¹ T. Park, M. B. Salamon, E. M. Choi, H. J. Kim, and S. -I. Lee, Phys. Rev. Lett. **90**, 177001 (2003). T. Park, E. E. M. Chia, M. B. Salamon, E. D. Bauer, I. Vekhter, J. D. Thompson, E. M. Choi, H. J. Kim, Sung-Ik Lee, and P. C. Canfield, cond-mat/0310663.
 - ¹² H. Aoki, T. Sakakibara, H. Shishido, R. Settai, Y. Onuki, P. Miranović, and K. Machida, J. Phys.: Condens. Matter **16**, L13 (2004).
 - ¹³ K. Deguchi, Z. Q. Mao, H. Yaguchi, and Y. Maeno, Phys. Rev. Lett. **92**, 047002 (2004) and cond-mat/0404070.
 - ¹⁴ T. Dahm, S. Graser, C. Iniotakis, N. Schopohl, Phys. Rev. B **66**, 144515 (2002).
 - ¹⁵ H. Kusunose, cond-mat/0405631.
 - ¹⁶ H. Kusunose, Phys. Rev. B **70**, 054509 (2004).
 - ¹⁷ M. Udagawa, Y. Yanase, M. Ogata, cond-mat/0408643.
 - ¹⁸ M. Udagawa, Y. Yanase, M. Ogata, cond-mat/0401206.
 - ¹⁹ P. Miranović, M. Ichioka, K. Machida, and N. Nakai, cond-mat/0312420.
 - ²⁰ P. Thalmeier, and K. Maki, Acta Physica Polonica B **34**, 557 (2003). K. Maki, H. Won, and S. Haas, Phys. Rev. B **69**, 012502 (2004).
 - ²¹ T. Watanabe, M. Nohara, T. Hanaguri, and H. Takagi, Phys. Rev. Lett. **92**, 147002 (2004).
 - ²² K. Izawa, K. Kamata, Y. Nakajima, Y. Matsuda, T. Watanabe, M. Nohara, H. Takagi, P. Thalmeier, and K. Maki, Phys. Rev. Lett. **89**, 137006 (2002).
 - ²³ P. Miranović, private communication.
 - ²⁴ K. Izawa, H. Yamaguchi, Y. Matsuda, H. Shishido, R. Settai, and Y. Onuki, Phys. Rev. Lett. **87**, 057002 (2001).
 - ²⁵ Y. Hasegawa, K. Machida, and M. Ozaki, J. Phys. Soc. Jpn. **69**, 336 (2000). Y. Hasegawa, and M. Yakiyama, J. Phys. Soc. Jpn. **72**, 1318 (2003).